Int j simul model 23 (2024) 1, 5-16
Original scientific paper

POST-BUCKLING OPTIMISATION OF COMPOSITE STRUCTURES USING A FIREFLY ALGORITHM

Koide, R. M.[*]; Herrera, P. H.[**]; Luersen, M. A.[**,#] & Ferreira, A. P. C. S.[**]
[*] Unicuritiba University Centre, Curitiba, PR, Brazil
[**] Department of Mechanical Engineering, Federal University of Technology – Parana, Curitiba, PR, Brazil
E-Mail: rubemkoide@hotmail.com, pherrera@alunos.utfpr.edu.br, luersen@utfpr.edu.br, apaula@utfpr.edu.br ([#] Corresponding author)

Abstract
In this work, a firefly algorithm was implemented and used to optimise composite structures in the post-buckling regime. In the first case studied, the goal was to maximise the post-buckling load of a rectangular plate subjected, independently, to shear load and uniaxial compression. The orientations of the layers served as design variables, while a maximal transverse displacement was considered as a constraint. Next, a reinforced flat panel was studied, with the goal of maximising the shear load in the post-buckling regime while constrained by the Tsai-Wu criterion. The design variables were the positions of the stiffeners and the orientations of the layers of the laminate. The degree of improvement in the maximum post-buckling load depended on the specific problem and ranged from 2.5 to 36 % compared to baseline designs. The selection of the structures chosen for the analyses ensured that the firefly algorithm was tested with progressively more challenging optimisation problems. The results suggested that the firefly algorithm could be used in the design of laminated composite structures.
(Received in April 2023, accepted in December 2023. This paper was with the authors 3 months for 2 revisions.)

Key Words: Laminated Composites, Post-Buckling, Stiffened Panel, Optimisation, Firefly Algorithm

1. INTRODUCTION

The use of fibre-reinforced laminates in different industrial sectors has increased rapidly in recent decades due to their high strength-to-weight ratio and ability to produce efficient, thin-walled structures. However, thin structures are prone to buckle, potentially causing structural problems. Since the buckling sensitivity of thin-walled laminates is higher, instability analyses are required to ensure their safety. This is done by determining their ultimate load in the post-buckling regime. Despite all the advances and knowledge already gained in this field [1-6], laminated structures' post-buckling behaviour is challenging to predict due to various influencing factors, such as ply orientation, shape, imperfections, thickness and material properties. Structural optimisation of composite materials has been the focus of many research groups in the last few years. For laminated composite structures, the usual approach is to look for the best stacking sequence that maximises the buckling or post-buckling load using an optimisation algorithm [7-11].

The firefly algorithm (FA) was introduced by Yang [12]. Since then, several researchers have proposed improvements and combinations with other heuristics to solve different kinds of problems ([13-17], among others). One of the first implementations of the discrete form of the firefly algorithm (DFA – discrete firefly algorithm) was done by Durkota [18], for the quadratic assignment problem (QAP). Later, Sayadi et al. [19] and Poursalehi et al. [20] successfully implemented DFAs and, respectively, used them to solve the manufacturing-cell-formation problem and optimise the fuel-loading pattern in a nuclear reactor. The literature review carried out as part of the present study found that FA and DFA are not yet widely applied in optimising laminated composite structures and could be a potential technique for this class of problem. In this work, a DFA is implemented and used to optimise rectangular plates with different aspect ratios under in-plane shear load and uniaxial compression. The goal is to find the optimum

stacking sequence that maximises the applied load under the constraint of a fixed prescribed maximum transverse displacement. The algorithm is also used to find the positions of the stiffeners and the stacking sequence that optimise the ultimate load of a stiffened composite flat panel in the post-buckling regime. The panel is subjected to an in-plane shear load, and the Tsai-Wu failure criterion is used as a constraint. The DFA is coded in Python, and the structures' response is obtained using an FEM model built in Abaqus.

2. THE FIREFLY ALGORITHM

The FA is a nature-inspired heuristic algorithm designed to solve optimisation problems. Fireflies produce small, rhythmical flashes of light, and the pattern in which these are produced is often unique to each species. The flashes, a form of bioluminescence, are produced by a biochemical process. Although most luminescent organisms produce only slow modulated flashes or glows, many species of adult fireflies are able to control their bioluminescence to emit intense, discrete flashes [21], which are used to attract partners and potential prey. The flashing-light behaviour of fireflies is very closely connected with the collective decisions of these insects and forms the basis of the FA. This algorithm assumes that each firefly observes its current position and tries to move to a source of light that is more intense than its own. Local and global searches take place in the form of firefly movements, and the choice of a local or global search depends on the intensity of the light emitted by the fireflies.

2.1 The structure of the firefly algorithm

The intensity of the light, I, from a source is inversely proportional to the square of the distance, r, from the source, i.e., $I \propto 1/r^2$. Hence, the intensity of the light from a firefly observed by another firefly decreases as the distance between two fireflies increases. Furthermore, as the distance increases, I also decreases because of the absorption of light by air. After studying the characteristics of the light emitted by fireflies, Yang formulated an algorithm inspired by the behaviour of these insects [12]. The algorithm is based on three rules: (i) a firefly's attractiveness is proportional to its brightness, both of which decrease with distance and for any two fireflies, the one with lower brightness will move toward the other; (ii) if a particular firefly does not shine or not emit flashes, its movement will be random; (iii) the brightness of a firefly is determined by the objective function, i.e., it is directly related to the objective function.

Pseudocode with the main procedures of the FA is shown in Fig. 1.

Input: $f(\boldsymbol{x}), \boldsymbol{x} = (x_1, x_2, \dots, x_{nr\_fly})$; // objective function
$nr\_fly, I_0, \gamma, \alpha$; // define initial constants
Output: $\boldsymbol{x}^{min}$; // optimized values of the design variables

For $i \leftarrow 1$ **to** nr_fly **do**
  $\boldsymbol{x}^i \leftarrow$ Initial_Solution();
End
While *criterion not satisfied* **do**;
  $min \leftarrow arg_{i\in\{1,\dots,m\}}\min\left(f(\boldsymbol{x}^i)\right)$;
  For $i \leftarrow 1$ **to** nr_fly **do**
    For $j \leftarrow 1$ **to** nr_fly **do**
      If $f(\boldsymbol{x}^i) < f(\boldsymbol{x}^j)$ **then** // move $\boldsymbol{x}^i$ para $\boldsymbol{x}^j$
        $r_{i,j} \leftarrow$Distance$(\boldsymbol{x}^i, \boldsymbol{x}^j)$;
        $\beta \leftarrow$Attractiveness$(I_0, \gamma, r_{i,j})$;
        $\boldsymbol{x}^i \leftarrow (1-\beta)\boldsymbol{x}^i + \beta\boldsymbol{x}^j + \alpha\left(Random() - \frac{1}{2}\right)$; // movement
      End
    End
  End
  $\boldsymbol{x}^{min} \leftarrow \boldsymbol{x}^{min} + \alpha\left(Random() - \frac{1}{2}\right)$; //best firefly moves randomly
End

Figure 1: Pseudocode of the firefly algorithm.

The parameters are as follows: nv represents the number of design variables; nr_fly is the number of fireflies; I_0 is the intensity of the light; γ is the absorption coefficient; β is the attractiveness; α is a random parameter used to improve the local search; r_{ij} is the distance between firefly i and firefly j; and x^i is the movement of firefly i toward a brighter firefly.

Reviews of the FA can be found in the references [12, 15, 22-24].

2.2 The discrete firefly algorithm applied to laminated composites

The FA was originally developed for continuous variables, and a discrete form, called the discrete firefly algorithm (DFA), was subsequently developed by [18]. The equation describing the movement of one firefly toward another due to the latter's attractiveness can be written as:

$$x_i \leftarrow (1-\beta)x_i\beta x_j + \alpha(\text{Random}(\,) - 0.5) \tag{1}$$

This was redefined by Durkota [18] as:

$$x_i \leftarrow \text{attractiveness}\,(x_i, x_j, \alpha, \beta) \tag{2}$$

The definition of attractiveness function for discrete variables requires solutions represented by permutations and their operations. The set of the initial population of fireflies, S_{np}, is obtained randomly with permutations (1, 2, …, np). The distance between two fireflies can be determined from the Hamming distance, which corresponds to the number of mismatched elements in two permutations [18]. For permutations π_1, π_2, $\pi_3 \in S_{np}$,

$$\begin{aligned} \pi_1 &= [1\ 2\ 3\ 4\ 5\ 6\ ] \\ \pi_2 &= [1\ 2\ 4\ 3\ 6\ 5\ ] \\ \pi_3 &= [1\ 2\ 4\ 5\ 6\ 3\ ] \end{aligned} \tag{3}$$

In Eq. (3), the Hamming distance (π_1,π_2) between π_1 and π_2 is 4, since only the first two elements are the same and the other four elements are mismatched.

The attractiveness, as defined by Eq. (1) for continuous variables and Eq. (2) for discrete variables, is dependent on β and α. This dependence can be rewritten by computing the movement initially as a function of β and then only as a function of α. This order must be respected as otherwise step α could move the firefly too close to, or far from, the original position, which would be an inefficient movement. Eq. (1) can thus be reformulated as:

$$\begin{aligned} x_i &\leftarrow (1-\beta)x_i\beta x_j \\ x_i &\leftarrow x_i + \alpha(\text{Random}(\,) - 0.5) \end{aligned} \tag{4}$$

As the algorithm proceeds from one iteration to the next, the distances between the fireflies tend to decrease. In other words, as the Hamming distance is being used, the number of equal elements should increase. To this end, step β begins with a check of the elements that are common to the permutations.

The firefly metaheuristic can be applied to composite materials as determination of the stacking sequence (layup) is a combinatorial optimisation problem. The stacking sequence of a composite laminate is defined by the orientations of the various layers and is usually symmetric and balanced. A laminate is said to be symmetric when the stacking sequence is symmetric with respect to the mid-plane of the laminate and balanced when for each $+\theta$ ply orientation there is a corresponding $-\theta$ ply (of the same material and thickness) somewhere in the laminate. The optimum sequence is the best stacking solution found for the specified objective function. The sequence is discrete as the variables (ply orientation angles) are discrete, typically with values of 0°, ±15°, ±30°, ±45° or 90°. Fig. 2, a schematic diagram of one iteration of the DFA applied to laminated composite structures, shows at which point of the algorithm the Hamming distance is calculated. Fig. 2 a represents the general DFA, and Fig. 2 b illustrates the application of the DFA to optimisation of the stacking sequence of laminated composite materials. The objective function, which must be maximised, is the post-buckling load.

First, the initial parameters of the algorithm (*nr_fly*, I_0, β_0, γ and α) are set. These parameters represent the number of initial solutions (*nr_fly*); the initial light intensity (I_0) which decreases as the distance between two fireflies increases; the initial attractiveness (β_0); the light absorption coefficient (γ); and the parameter α, which is used in local and global searches.

The initial set of solutions is randomly generated. Determining the light intensity for each of these solutions is equivalent to calculating the objective function for the corresponding stacking sequences. As the Hamming distance can be difficult to determine and steps β and α difficult to implement using the values of the discrete variables $\{0_2, \pm15, \pm30, \pm45, \ldots, 90_2\}$), these are coded as integers from one to five. Once the Hamming distance is known, the attractiveness of the fireflies can be calculated. The attractiveness index enables a local search to be performed and the movement of a firefly to be determined according to step β. A global search is then performed as shown in step α using a random disturbance. Together, these two procedures give the complete movement of the firefly for each iteration of the algorithm. The best solution found in this way is stored and reviewed after each iteration until a stopping criterion is satisfied. Typically, this is a given number of iterations or calculations of the objective function.

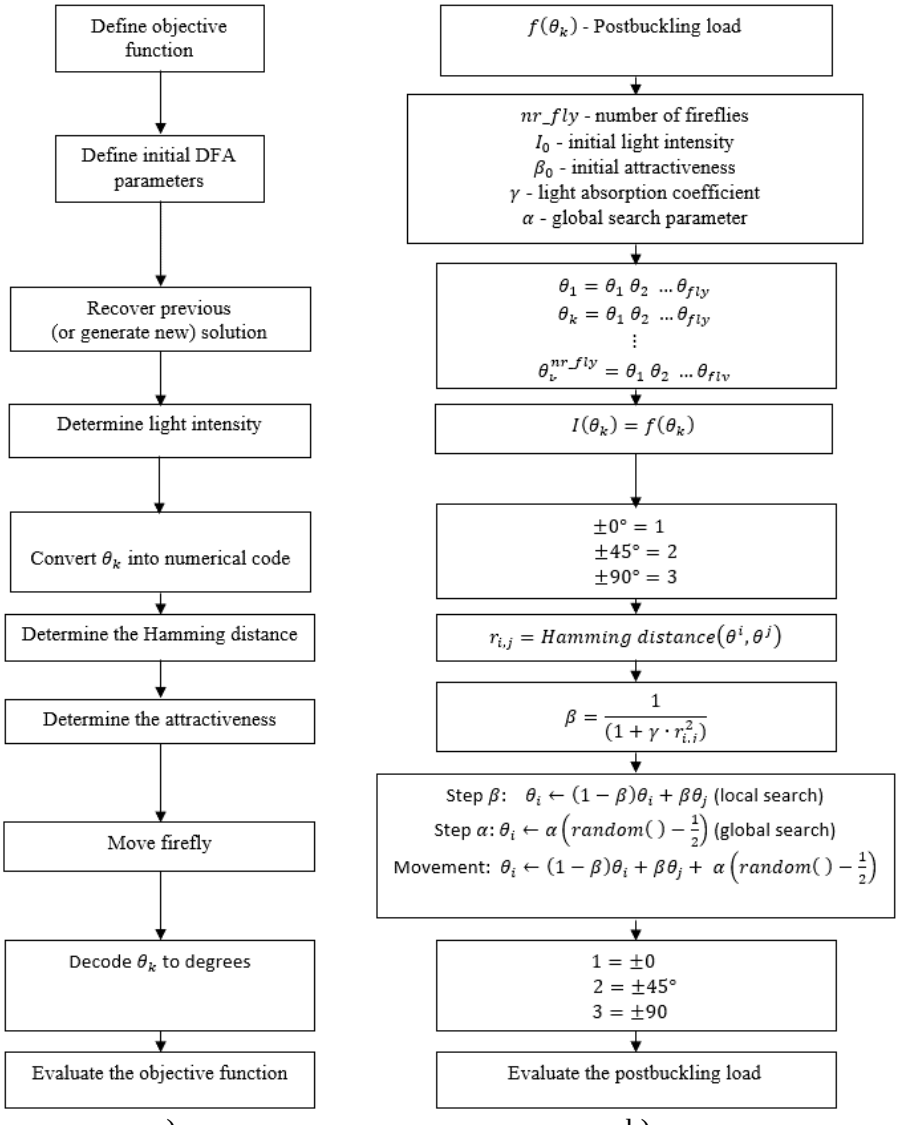

Figure 2: Flowchart of one iteration of the firefly algorithm: a) general DFA, b) application of the DFA to optimisation of the layup of laminated composite structures.

3. POST-BUCKLING MODELLING AND OPTIMISATION WITH DFA

The models presented here were first validated with solutions found in the literature. The structures were then optimised using DFA so that the performance of the algorithm when used to optimise composite structures in the post-buckling regime could be analysed.

3.1 Case 1 – Plate under shear load and uniaxial compression

For the first case analysed, the geometries of the laminated plates, the boundary conditions and the coordinate system are shown in Fig. 3. The length and width of the plate are a and b, respectively, and θ represents the angle between the fibres and the x_1 axis for a specific ply. For the SS plate under shear loading, we also constrained the rotation around the x_3 axis (perpendicular to the x_1-x_2 plane) at the central point.

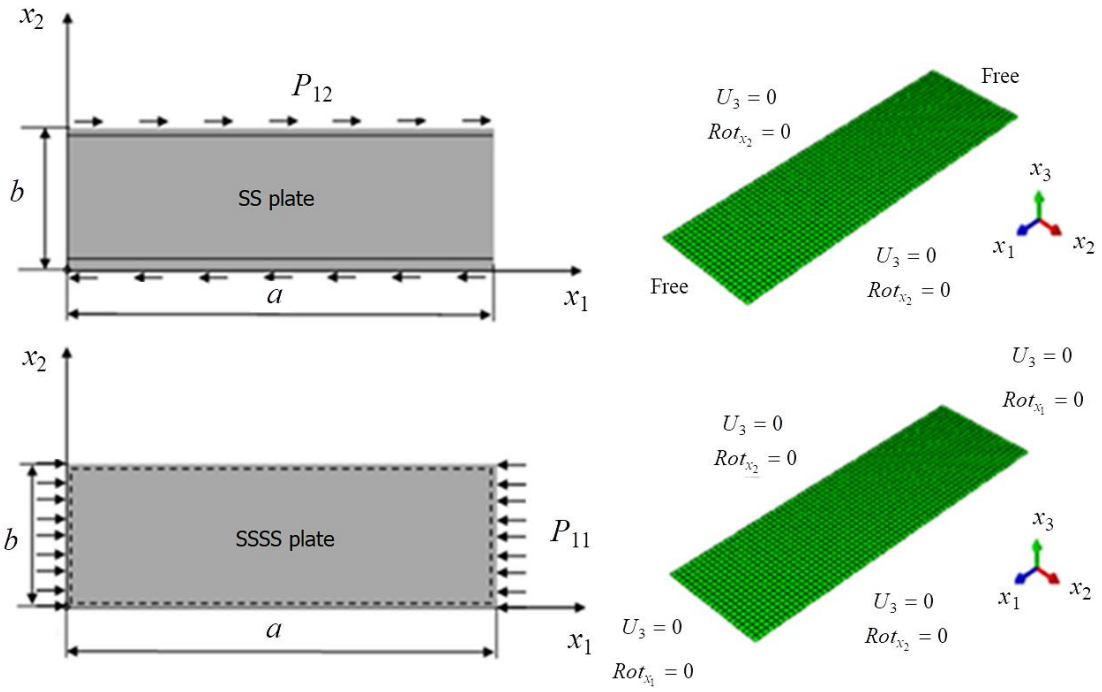

Figure 3: Plate geometry, loads, boundary conditions and finite element meshes. U_i represents the constrained displacement in the x_i direction, and Rot_{xi} the constrained rotation around the x_i axis.

The FEM models were built in Abaqus using four-node shell elements (S4R) with six degrees of freedom per node. The element length was kept constant at 10 mm. In the first case (SS plate under shearing), the edges under shearing were simply supported, while the other two edges were free. In the second case (SSSS plate under uniaxial compression), all the edges were simply supported. The FEM models were validated by comparing the results predicted by the models with those reported in [3] and [4]. The validation models were symmetric, balanced laminates with the stacking sequence given by $[0 / 90 / 90 / 0 / 90]_s$ for the SS plate and $[0 / 90 / 0 /90]_s$ for the SSSS plate. The elastic properties of the plies, which were 0.184 mm thick, were $E_1 = 157$ GPa, $E_2 = 8.5$ GPa, $G_{12} = 4.2$ GPa and $\nu_{12} = 0.35$. The dimensions of the plates used for the validation in both cases were $a = 640$ mm and $b = 200$ mm. Fig. 4 shows a comparison of the shear load vs. displacement curves for the SS plate (shear loading); there is satisfactory agreement between the curves up to a transverse displacement of 2 mm. In the case of the SSSS plate (uniaxial compression), comparison of the results also reveals satisfactory agreement between the curves. The differences between the results in the large-displacement region in both cases can be explained by the fact that different kinds of nonlinear analyses were used in this study and the studies by [3, 4].

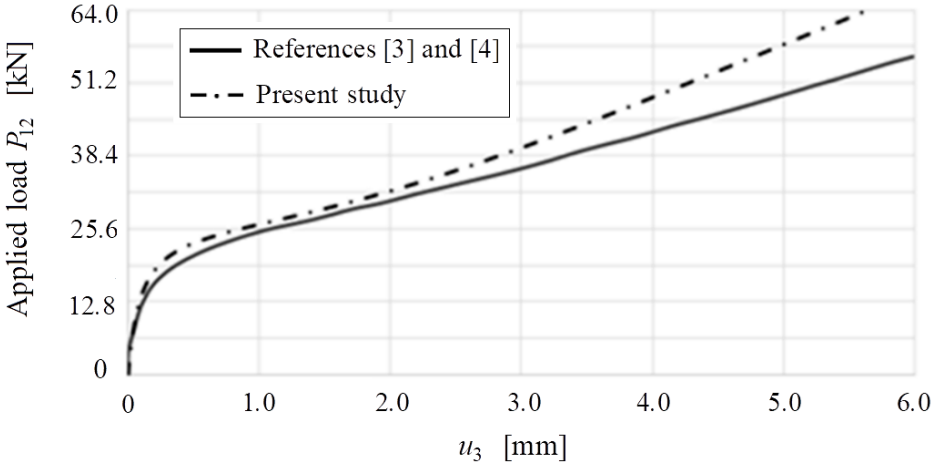

Figure 4: Post-buckling curves (load vs. displacement) for validation of the SS plate under shear loading.

The first step of the analysis was to predict the buckling mode shapes with a simple linear perturbation "buckle" analysis. The resulting mode shapes were used to introduce imperfections into the model, the amplitudes of which were set to 10 % of the plate thickness. To perform the nonlinear analysis (including analysis of the post-buckling behaviour), a static general step with a stabilization coefficient was used. In the second step, prescribed displacements were applied at the horizontal edges, and the corresponding post-buckling loads (P_{11} – uniaxial compression; P_{12} – shearing, given in N or kN) were obtained by finite element analysis.

The optimisation problem can be formulated as follows:

$$\begin{aligned} &\text{Find: } \theta_k,\ \theta_k \in \{0_2, \pm 15, \pm 30, \pm 45,\ 90_2\}, k = 1, \ldots, n \\ &\text{Maximise: } P_{11} \text{ or } P_{12} \text{ (post-buckling load)} \\ &\text{Subject to: maximum 2 mm transversal displacement,} \end{aligned} \tag{5}$$

where θ_k denotes the orientation angle of two contiguous plies, k is the stacking sequence index and n (= 16) is half the total number of layers. The criterion of a maximum transverse displacement of 2 mm was chosen to ensure that the load would be in the post-buckling region.

To set the initial parameters for the DFA algorithm, many tests were performed using the model with an aspect ratio a/b = 3.4 and 32 plies. The other parameters used included β = 0.8 and α = 1. The number of fireflies recommended in the literature is between 20 and 50 [14]. Here, satisfactory convergence was found using 40 fireflies.

The critical load and maximum transverse displacement versus the number of objective-function evaluations are shown in Fig. 5 for the SS plate with an aspect ratio a/b = 3.4 and 32 plies. Each I_j (j = 1, …, 6) indicates an independent run. The load increases as the number of objective-function evaluations increases, as expected, and converges after 8000 evaluations. The maximum transverse displacement varies from 2 to 2.089 mm. The displacement constraint is slightly violated because the algorithm is incremental, making it difficult to ensure an exact displacement of 2 mm.

Numerical tests were carried out to determine the initial parameters, including the number of fireflies and objective-function evaluations. Based on the results of these tests, fixed values of 10000 objective-function evaluations n_e and 40 fireflies were adopted for all the analyses. Optimisations of three plates with aspect ratios (a/b) of 2.2, 3.4 and 5.2 were then performed for each load configuration. The results of these optimisations are summarized in Table I. For the purposes of comparison, Table II shows the post-buckling load for symmetric angle-ply laminates.

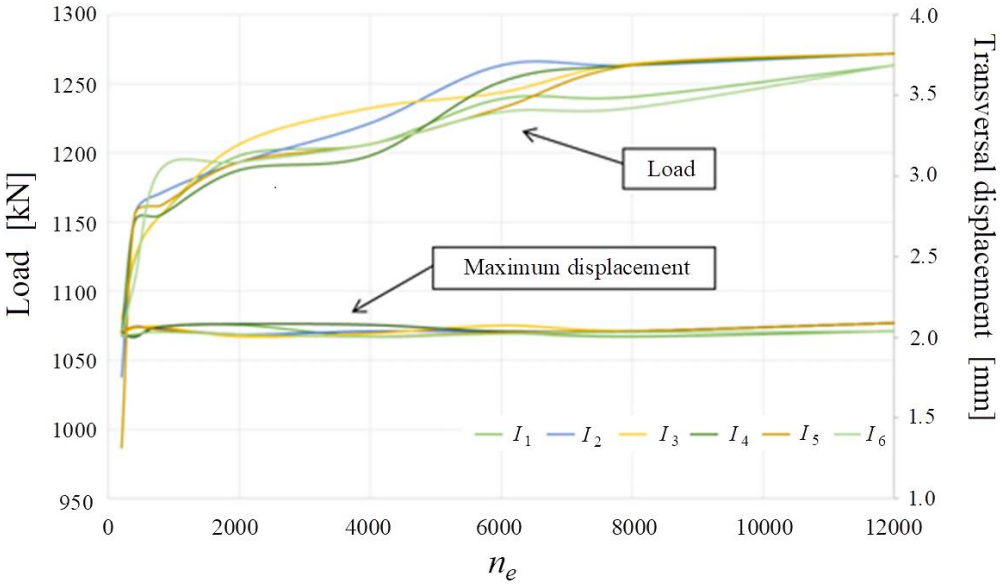

Figure 5: Convergence of the FA: applied load versus number of objective-function evaluations (n_e) for the shear load and a/b = 3.4 (six independent runs: I_1 to I_6).

Table I: Results of post-buckling optimisation with the FA.

a/b	**Load** (kN)	**Stacking sequence**
Shear load		
2.2	1288	$[\pm 45_6 / \pm 15_2]_s$
3.4	1271	$[\pm 30_2 / \pm 45_4 / \pm 15_2]_s$
5.2	1120	$[\pm 45 / 90_2 / 0_2 / \pm 45 / 0_2 / \pm 30 / \pm 15 / 0_2]_s$
Compressive load		
2.2	268	$[\pm 45_6 / \pm 15_2]_s$
3.4	265	$[\pm 45_4 / \pm 30_2 / \pm 15_2]_s$
5.2	264	$[\pm 45_6 / 90_4]_s$

Table II: Post-buckling load for symmetric angle-ply laminates.

a/b	**Stacking sequence**				
	$[0]_{32}$	$[\pm 15_8]_s$	$[\pm 30_8]_s$	$[\pm 45_8]_s$	$[90]_{32}$
	Shear load (kN)				
2.2	960	1139	1176	1200	332
3.4	730	1068	1107	1098	243
5.2	670	794	904	803	194
	Compressive load (kN)				
2.2	83	123	216	261	99
3.4	82	123	215	259	97
5.2	80	122	215	258	95

The results for the different aspect ratios show, as is already well known, that the post-buckling load increases as the ratio a/b decreases. In the case of the shear load, the 90° orientation appears only once, suggesting that it is more advantageous to use the other orientations. This is corroborated by Table II, which shows that the 90° orientation tends to reduce the ultimate load compared with angle-ply laminates with ± 30° and ± 45°orientations. The same tendency was observed with the compressive load, but for 0° and 90° orientations.

For the compressive load configuration with angle-ply laminates, the ± 45° orientation yielded the best results regardless of the aspect ratio of the plate. The ± 30° orientation resulted in a high load capability, as also observed with the shear load. The worst performance with the compressive load was observed for 0°. The optimum stacking sequences identified by the algorithm were combinations of ±45° and ±15° orientations for the smallest aspect ratio and combinations of ±45° and 90° for an aspect ratio of 5.2, the 90° plies being positioned internally between the ±45°plies.

The DFA maximised the post-buckling load in all the cases analysed. In the case of the SS plate (shearing) the increase in post-buckling load compared with the symmetric angle-ply laminates was 7.3 %, 14.8 % and 23.9 % for aspect ratios of 2.2, 3.4 and 5.2, respectively. For the SSSS plate (uniaxial compression), the increase was much smaller, approximately 2.5 % for all the aspect ratios tested.

The literature recommends the use of no more than four contiguous plies with the same orientation to avoid delamination and manufacturing problems. However, as the main purpose of the present work was to evaluate the performance of the FA when used to design the layup of laminated composite plates, this constraint was not considered in the formulation of the optimisation problem.

3.2 Case 2 – Optimisation of the position of the stiffeners in a flat panel

The chosen structure for case 2, which is based on [25] and depicted in Fig. 6, was composed of a flat, square shell measuring 762 mm × 762 mm and six stiffeners 762 mm long and 34.34 mm high. The blade-stiffened panel was simply supported on all edges, and different scenarios were considered for the model validation. The panel was subjected to uniaxial compression in the x direction (N_x) and an in-plane shear load (N_{xy}), where N_x and N_{xy} represent resultant forces, i.e., forces per unit length, commonly employed in shell analysis. For the optimisation study, we focused solely on shear loading. The panel was modelled with 1296 Abaqus S8R elements (see Fig. 6), which are eight-node shell elements with six degrees of freedom per node.

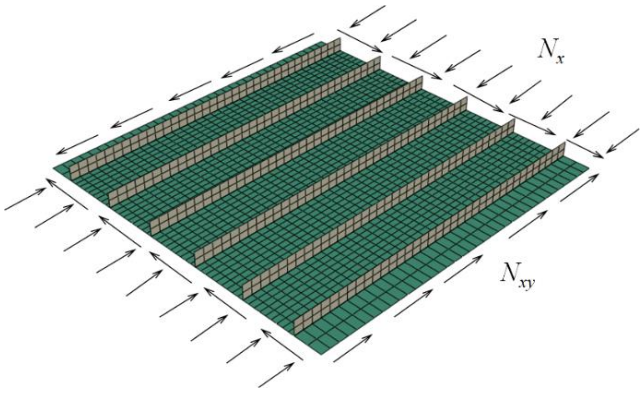

Figure 6: Finite element model of the stiffened panel.

The material properties of the composite plies used in the validation model were E_1 = 131 GPa, E_2 = 13 GPa, ν_{12} = 0.38 and G_{12} = 6.41 GPa. The stacking sequences of the skin and stiffeners were $[45 / -45 / -45 / 45 / 0 / 90]_S$ and $[45 / -45 / -45 / 45 / 0]_S$, respectively.

The buckling load factors obtained in this work are shown in Table III, where they can be compared with those provided by [25]. There is good agreement between the values in both studies for all the load combinations analysed. The largest difference is 2.56 %, for pure shear, while the smallest is 0.50 %, for pure compression.

To optimise the panel, additional material properties not available in [25] are required because the Tsai-Wu criterion is applied as a constraint. Accordingly, the elastic and strength

properties were taken from [26] and are shown in Table IV. In addition, the number of plies was increased from 12 to 32; all the plies were 0.150 mm thick.

Table III: Results of validation of the FEM model.

Load (N/mm)		**Buckling load factor**		
N_x	N_{xy}	Reference [25]	Present study	Difference (%)
0	175.1	1.553	1.513	2.58
-87.6	175.1	1.206	1.185	1.74
-175.1	175.1	0.840	0.832	0.95
-175.1	0	1.003	0.998	0.50

Table IV: Material properties of the IM7/8552 unidirectional carbon tape used for the panel.

Elastic property (unit)	**Value**	**Strength property** (unit)	**Value**
E_{11} (GPa)	145	X_T (MPa)	2414
E_{22} (GPa)	8.9	X_C (MPa)	1365
ν_{12} (-)	0.33	Y_T (MPa)	51
G_{12} (GPa)	5.6	Y_C (MPa)	269
G_{13} (GPa)	5.6	S_{12} (MPa)	120
G_{23} (GPa)	4.48		

The connections between the skin and stiffener elements were made with the *TIE command in Abaqus, which makes the translations and rotations of the elements between two surfaces equal, resulting in a single part.

The finite element analysis was divided into two stages. First, a linear buckling analysis was performed to find the buckling modes, and the first three buckling-mode shapes were introduced into the model as geometric imperfections with amplitudes of 10 %, 1 % and 0.1 % of the thickness of the laminate. Then, a large-displacement nonlinear analysis was performed to determine the maximum load without failure according to the Tsai-Wu criterion.

In this case, the positions of the four internal stiffeners were optimised and the two in the outer positions were fixed 63.5 mm from the edges. The domain of the stiffener positions was discretized so that there was no overlap between them, and each stiffener could occupy one of 11 possible positions, as shown in Fig. 7.

The layup of the skin is $[\pm 45 / \mp 45 / 0 / 90 / 0_2 / \pm 45_2 / 90_2 / 0_2]_S$.

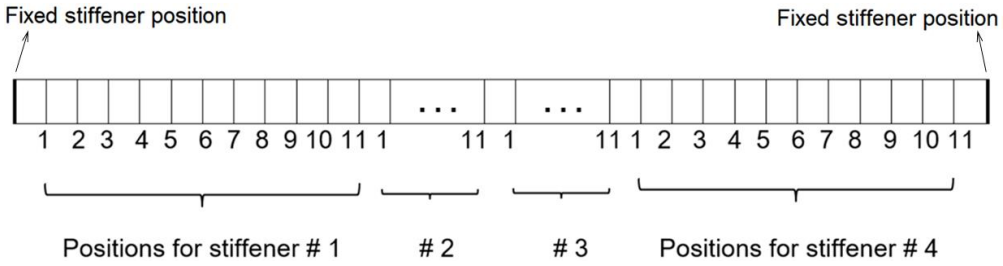

Figure 7: Possible stiffener positions.

The optimisation problem can be formulated as follows:

$$\begin{aligned} &\text{Find: } X_k, \quad X_k \in \{1,2,3,\ldots,11\}, k = 1,\ldots,n_s \\ &\text{Maximise: } N_{xy_{\max}} \text{ (maximum shearing load in post-buckling regime)} \\ &\text{Subject to: Tsai-Wu failure criterion} \end{aligned} \tag{6}$$

where X_k represents the position of the stiffeners, k the sequence index and n_s the number of stiffener positions to be optimised.

For this problem, the population consisted of 10 fireflies, and the algorithm parameters γ and α were set to 0.8 and 1, respectively. A total of 1000 objective-function evaluations were used as the stopping criterion.

The results are shown in Table V and are compared with the configuration used to validate the model, i.e., all stiffeners equally spaced. A study of the convergence robustness of the algorithm was also performed by comparing the results obtained in five different runs of the algorithm, as shown in Fig. 8.

Table V: Results of the optimisation – case 2.

Description	**Positions of the stiffeners**	$N_{xy_{max}}$ (N/mm)
Baseline configuration	[9 7 5 3]	513.245
Optimised configuration	[11 9 4 2]	584.702

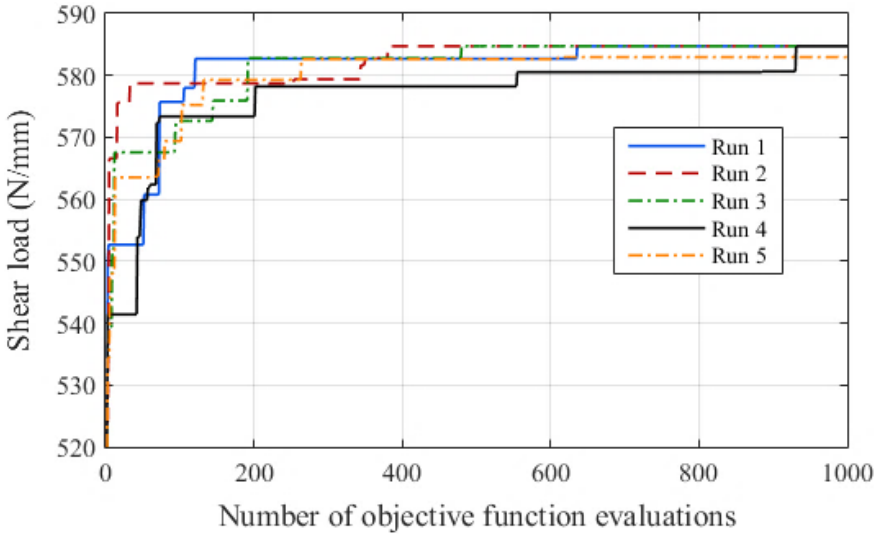

Figure 8: Convergence of the DFA: maximum post-buckling load versus number of objective-function evaluations for five independent runs.

3.3 Case 3 – Optimisation of the position of the stiffeners and the stacking sequence for a flat panel

In this case, the same structure of case 2 is studied, however, the stacking sequence of the skin was also optimised. This implies a large number of design variables, making the problem more complex. The number of fireflies was therefore increased to 50, as recommended by [14], and the number of objective-function evaluations was increased to 1500. The other parameters (a and g) were kept the same as in case 2. The optimisation problem can be formulated as:

$$\begin{aligned} &\text{Find: } X_k, \quad X_k \in \{1,2,3,\ldots,11\}, k = 1,\ldots,n_s \\ &\qquad \theta_j, \quad \theta_j \in \{0,\pm 45,90_2\}, j = 1,\ldots,n_l \\ &\text{Maximise: } N_{xy_{\max}} \text{ (maximum shearing load in post-buckling regime)} \\ &\text{Subject to: Tsai-Wu failure criterion} \end{aligned} \tag{7}$$

where θ_j is the ply orientation and n_l the number of plies to be optimised. As the laminate was assumed to be symmetric and balanced, the number of angles to be determined was reduced from 32 to 8, and as a design constraint, the possible orientations were restricted to 0º, 45º and 90º. The options for the positions of the stiffeners were kept the same as in case 2. The results for this case are summarized in Table VI, where it can be seen that the post-buckling load for the optimised configuration is 36 % higher than for the baseline configuration.

Table VI: Results of the optimisation – case 3.

Description	Stacking sequence	Positions of the stiffeners	$N_{xy_{max}}$ (N/mm)
Baseline configuration	$[\pm 45 / \mp 45 / 0_2 / 90_2 / \pm 45_2 / 90_2 / 0_2]_s$	[9 7 5 3]	513.245
Optimised configuration	$[\, 90_4 / \pm 45 / 90_2 \,/\, \pm 45_3 / 0_2 \,]_s$	[11 8 3 2]	701.540

4. CONCLUSION

The main goal of this work was to test the use of the DFA to optimise the layup of laminated composite plates and flat and curved panels with stringers so as to maximise the post-buckling load. To analyse the post-buckling behaviour, FEM models were created in Abaqus and connected to the optimisation algorithm, which was coded in Python. Convergence and validation tests were carried out. In case 1, which focused on laminated plates, both compressive and shear loads were analysed to identify the best stacking sequence. Plates with three different aspect ratios and different load configurations were optimised. When a shear load was applied, the optimised post-buckling load was around 7 % to 24 % higher than for symmetric angle-ply laminates. With a compressive load, the increase was much lower, around 2.5 %. In cases 2 and 3 the positions of the stiffeners on a flat panel under shear loading and the stacking sequence were optimised to maximise the post-buckling load. The Tsai-Wu failure criterion was used as a constraint. In case 2, only the positions of the stiffeners were considered as design variables. The results showed a 14 % increase in the maximum post-buckling load compared with the baseline configuration. In case 3, both the positions of the stiffeners and the stacking sequence were optimised. The increase in post-buckling load in this case, using the same baseline configuration as in case 2, was 36 %.

The results presented here confirm that DFA is an alternative optimisation method that can be successfully applied to the design of laminated composite structures. Future investigations could further explore optimization in different types of composite structures or under more complex loading conditions. Moreover, integrating DFA with other optimization techniques may yield additional improvements.

Despite the encouraging outcomes, it is crucial to acknowledge the limitations of the method employed. The selection of Tsai-Wu as the failure criterion may not comprehensively cover all aspects of failure behaviour. Other criteria and structural reliability analyses could be considered for future studies.

REFERENCES

[1] Hutchinson, J. W.; Koiter, W. T. (1970). Postbuckling theory, *Applied Mechanics Reviews*, Vol. 23, No. 12, 1353-1366

[2] Pandey, M. D.; Sherboune, A. N. (1993). Postbuckling behaviour of optimized rectangular composite laminates, *Composite Structures*, Vol. 23, No. 1, 27-38, doi:10.1016/0263-8223(93)90071-W

[3] Mittelstedt, C.; Schröder, K.-U. (2010). Postbuckling of compressively loaded imperfect composite plates: closed-form approximate solutions, *International Journal of Structural Stability and Dynamics*, Vol. 10, No. 4, 761-778, doi:10.1142/S0219455410003725

[4] Mittelstedt, C.; Erdmann, C.; Schröder, K.-U. (2011). Postbuckling of imperfect rectangular composite plates under inplane shear closed-form approximate solutions, *Archive of Applied Mechanics*, Vol. 81, No. 10, 1409-1426, doi:10.1007/s00419-010-0491-y

[5] Novoselac, S.; Ergić, T.; Baličević, P. (2012). Linear and nonlinear buckling and post buckling analysis of a bar with the influence of imperfections, *Technical Gazette*, Vol. 19, No. 3, 695-701

[6] Xu, X.; Carrera, E.; Yang, H.; Daneshkhah, E.; Augello, R. (2022). Evaluation of stiffeners effects on buckling and post-buckling of laminated panels, *Aerospace Science and Technology*, Vol. 123, Paper 107431, 13 pages, doi:10.1016/j.ast.2022.107431

[7] Le Riche, R.; Haftka, R. T. (1993). Optimization of laminate stacking sequence for buckling load maximization by genetic algorithm, *AIAA Journal*, Vol. 31, No. 5, 951-956, doi:10.2514/3.11710

[8] Aymerich, F.; Serra, M. (2008). Optimization of laminate stacking sequence for maximum buckling load using the ant colony optimization (ACO) metaheuristic, *Composites Part A: Applied Science and Manufacturing*, Vol. 39, No. 2, 262-272, doi:10.1016/j.compositesa.2007.10.011

[9] Bloomfield, M. W.; Herencia, J. E.; Weaver, P. M. (2010). Analysis and benchmarking of meta-heuristic techniques for lay-up optimization, *Computers & Structures*, Vol. 88, No. 5-6, 272-282, doi:10.1016/j.compstruc.2009.10.007

[10] Koide, R. M.; França, G. V. Z.; Luersen, M. A. (2013). An ant colony algorithm applied to lay-up of laminated composite plates, *Latin American Journal of Solids and Structures*, Vol. 10, No. 3, 491-504, doi:10.1590/S1679-78252013000300003

[11] Jing, Z.; Sun, Q.; Zhang, Y.; Liang, K. (2021). Stacking sequence optimization for maximum buckling load of simply supported orthotropic plates by enhanced permutation search algorithm, *Engineering Optimization*, Vol. 53, No. 10, 1695-1714, doi:10.1080/0305215X.2020.1818736

[12] Yang, X.-S. (2009). Firefly algorithms for multimodal optimization, Watanabe, O; Zeugmann, T. (Eds.), *Stochastic Algorithms: Foundations and Applications (SAGA 2009)*, Springer, Berlin, 169-178, doi:10.1007/978-3-642-04944-6_14

[13] Azad, S. K.; Azad, S. K. (2011). Optimum design of structures using an improved firefly algorithm, *International Journal of Optimization in Civil Engineering*, Vol. 1, No. 2, 327-340

[14] Gandomi, A. H.; Yang, X.-S.; Talatahari, S.; Alavi, A. H. (2013). Firefly algorithms with chaos, *Communications in Nonlinear Science and Numerical Simulation*, Vol. 18, No. 1, 89-98, doi:10.1016/j.cnsns.2012.06.009

[15] Tuba, M.; Bacanin, N. (2014). Improved seeker optimization algorithm hybridized with firefly algorithm for constrained optimization problems, *Neurocomputing*, Vol. 143, 197-207, doi:10.1016/j.neucom.2014.06.006

[16] Mao, C. L. (2021). Production management of multi-objective flexible job-shop based on improved PSO, *International Journal of Simulation Modelling*, Vol. 20, No. 2, 422-433, doi:10.2507/IJSIMM20-2-CO11

[17] Wang, M. (2021). Manufacturing capacity evaluation of smart job-shop based on neural network, *International Journal of Simulation Modelling*, Vol. 20, No. 4, 778-789, doi:10.2507/IJSIMM20-4-CO19

[18] Durkota, K. (2011). *Implementation of a Discrete Firefly Algorithm for the QAP Problem within the SEAGE Framework*, Bachelor Thesis, Czech Technical University, Prague

[19] Sayadi, M. K.; Hafezalkotob, A.; Naini, S. G. J. (2013). Firefly-inspired algorithm for discrete optimization problems: an application to manufacturing cell formation, *Journal of Manufacturing Systems*, Vol. 32, No. 1, 78-84, doi:10.1016/j.jmsy.2012.06.004

[20] Poursalehi, N.; Zolfaghari, A.; Minuchehr, A. (2013). Multi-objective loading pattern enhancement of PWR based on the discrete firefly algorithm, *Annals of Nuclear Energy*, Vol. 57, 151-163, doi:10.1016/j.anucene.2013.01.043

[21] Fister, I.; Fister Jr., I.; Yang, X.-S.; Brest, J. (2013). A comprehensive review of firefly algorithms, *Swarm and Evolutionary Computation*, Vol. 13, 34-46, doi:10.1016/j.swevo.2013.06.001

[22] Tilahun, S. L.; Ngnotchouye, J. M. T. (2017). Firefly algorithm for discrete optimization problems: a survey, *KSCE Journal of Civil Engineering*, Vol. 21, No. 2, 535-545, doi:10.1007/s12205-017-1501-1

[23] Li, J.; Wie, X.; Li, B.; Zeng, Z. (2022). A survey on firefly algorithms, *Neurocomputing*, Vol. 500, 662-678, doi:10.1016/j.neucom.2022.05.100

[24] Rezaei, K.; Rezaei, H. (2022). An improved firefly algorithm for numerical optimization problems and it's application in constrained optimization, *Engineering with Computers*, Vol. 38, No. 4, 3793-3813, doi:10.1007/s00366-021-01412-9

[25] Stroud, W. J.; Greene, W. H.; Anderson, M. S. (1984). *Buckling loads of stiffened panels subjected to combined longitudinal compression and shear: results obtained with PASCO, EAL, and STAGS computer programs*, NASA Technical Paper 2215, Langley Research Center, NASA, Hampton

[26] Araico, J. A.; Alberdi, I. O. Z.; Arribas, F. R. (2010). Postbuckling degradation FE analysis of stiffened composite panels, *International Journal of Structural Stability and Dynamics*, Vol. 10, No. 4, 645-668, doi:10.1142/S021945541000366X